Adsorption of Cr(VI) from aqueous solutions onto activated pomegranate peel waste

E.A. Abdel-Galil*, L.M.S. Hussin, W.M. El-Kenany

Hot Laboratories and Waste Management Center, Atomic Energy Authority, 13759 Cairo, Egypt, Tel. +201159895618; Fax: 20 244620784; email: ezzat_20010@yahoo.com (E.A. Abdel-Galil)

ABSTRACT

The present study deals with the employ of the chemically activated pomegranate peel (PGP-1N H_2SO_4) as a low-cost adsorbent for the retention of Cr(VI) ions from aqueous solutions. The physicochemical characteristics of the chemically activated pomegranate peel were studied using Fourier transform infrared spectroscopy, powder X-ray diffraction, thermogravimetric analysis, and scanning electron microscopy. The influences of several factors such as contact time, pH of the solution, initial concentration of the adsorbate ion, and adsorbent mass on the removal of Cr(VI) ions were studied using the batch sorption technique. The equilibrium data fitted reasonably well to the Langmuir model, while pseudo-second-order best designated the kinetics of the adsorption process. The maximum adsorption capacity for Cr(VI) ions onto pomegranate peel as calculated by the Langmuir model was found to be 28.28 mg/g at 25°C ± 1°C. The values of thermodynamic parameters ($\Delta G°$, $\Delta H°$, and $\Delta S°$) were computed from the Van't Hoff plot which revealed that the adsorption of Cr(VI) was feasible, endothermic, and spontaneous. Based on good uptake capacity, PGP-1N H_2SO_4 was successfully used for the removal and recovery of Cr(VI) from double-distilled water (DDW), tap water, synthetic seawater, natural seawater, and wastewater. The adsorbed metals were easily recovered by desorption in 0.5 N NaOH.

Keywords: Activated pomegranate peel; Adsorption; Cr(VI); Wastewater; Saline water; Isotherms; Kinetics

1. Introduction

The existence of heavy metal ions from the transition series, viz, Pb, Cu, Ni, Fe, Cr, etc., in the environment is of most important due to their hazardous effect to many life forms. Many organic pollutants are liable to biological decomposition but metal ions have a constant behavior, where they do not decompose into poisonous end products [1,2]. The contamination of aqueous waste stream by heavy metals is derived from many industrial activities such as mining, painting, metal plating, tanneries, manufacturing of car radiator, as well as fertilizers and fungicidal spray.

The most common oxidation states for chromium are Cr(III) and Cr(VI), the chemical properties of each of them are quite different. Cr(VI) can be converted to Cr(III) and vice versa depending on pH, the existence of oxidizing and

reducing agents, redox potential, the kinetics of the redox reactions, and the total chromium concentration in soil, water, and atmospheric systems [3]. The hazardous effects of different oxidation states of chromium depend upon its degree of solubility and mobility. Cr(III) does an important responsibility in the metabolism process of living organisms, quite insoluble and thus, can be easily precipitated out. As a result, it is less harmful. But the high concentration of Cr(III) is also dangerous [4,5]. Cr(VI) form needs more attention due to its high toxicity compared to Cr(III) form. The quite solubility of Cr(VI) causes many harmful effects such as diarrhea, liver infection, preventing germination of seeds, chlorosis of the plant leaves, etc [5–9]. It is also well-known to be mutagenic and carcinogenic. Strong exposure to Cr(VI) causes cancer in the digestive tract and lungs and may cause epigastric pain, nausea, vomiting, severe diarrhea, and hemorrhage [10]. Cr(VI) can pass through the cell membrane and there occurs the reduction of Cr(VI) to

* Corresponding author.

Cr(III). The reduced Cr(III) binds to the phosphate group of the DNA and stops its replication and transcription thus, destructive the cell and finally leads to the cell's death [11–14]. The harmful effect of Cr(VI) can be reduced via its conversion to Cr(III) by using micro-organisms [15,16]. In an aqueous solution, the Cr(VI) exists in various forms depending upon pH, such as chromate (CrO_4^{2-}), dichromate ($Cr_2O_7^{2-}$), or hydrogen chromate ($HCrO_4^{2-}$). CrO_4^{2-} is predominant in basic solutions, H_2CrO_4 is predominant at pH < 1, while $HCrO_4^{2-}$, and $Cr_2O_7^{2-}$ are predominant at pH 2–6 [2,17]. In Russian Federation, the official standards for maximum permissible limits (MPL) for chromium in drinking and domestic water, are 0.05 and 0.5 mg/L for Cr(VI) and Cr(III), respectively. The EU standards imply 0.5–5 mg/L and 0.1–0.5 mg/L for Cr(III) and Cr(VI), respectively [18,19].

Due to these adverse effects, chromium must be drastically removed from wastewater before it infiltrated into the surrounding medium or needs to be converted to less toxic forms [20]. Various techniques have been used for the scavenging of Cr(VI) from aqueous solutions including chemical precipitation, adsorption, ion exchange, electrocoagulation, membrane separation, and electrodialysis [2,5,17,21–26]. However, most of these techniques have many disadvantages including incomplete metal sorption, use of costly tools, energy requirements, and production of poisonous sludge and other disposal waste products [27]. In comparison adsorption technique is the lowest in economic cost, simple to operate, solves the challenge of sludge disposal, and an effective technique for the removal of Cr(VI) and other toxic elements [3,27–29]. Recently, researchers directed their attention to using low-cost adsorbents to remove Cr(VI) from wastewater. Among these adsorbents clays [30,31], industrial by-products [32], agricultural wastes [33], biomass [34], and polymeric materials [35], and young vesicular volcanic rocks [36]. Pomegranate peel discarded as a pollutant residue that can be used as a low cost and renewable source of biomass. It a by-product of the pomegranate juice industry is therefore a cheap and constitutes 5%–15% of its total weight [37]. In recent years, some researches used pomegranate peel to treat the wastewater samples from Cr(VI), Pb(II), and congo red [38–40]. The agricultural products and by-products contain cellulose, lignin, pectin, and many other compounds that have potential functional groups such as hydroxyl, carbonyl, amino, carboxylic, and alkoxy, which have a high affinity for the metal ions [41]. Before the chemical treatment, the pores of cellulose fibers are occupied with many viscous compounds such as lignin and pectin and this hinders the adsorption of metal ions. The activation process eliminates such compounds and the pores of cellulose fibers become vacant and available for binding with adsorbate ions, accordingly the adsorption capacities of agricultural adsorbents are enhanced after the chemical treatment [42,43]. This activation process has two different techniques, physical and chemical activation. Chemical activation is known as a single-step method of preparation activated carbon using chemical activating agents such as zinc chloride, sodium hydroxide, potassium hydroxide, sodium carbonate, hydrochloric acid, nitric acid, sulfuric acid, phosphoric acid, etc. Physical activation carried out via the carbonization of carbonaceous materials followed by activation of the resultant char using activating agents such as steam [44].

The present paper is concerned with the synthesis of activated carbons derived from pomegranate peel by chemical activation with NaOH, HNO_3, H_2SO_4, and HCl. The chemically modified pomegranate peel carbon (PGP-1N H_2SO_4) has been characterized by Fourier transform infrared (FT-IR), scanning electron microscopy (SEM), thermogravimetric analysis (TGA), and X-ray diffraction (XRD) techniques. It was employed as a low-cost adsorbent for the retention of toxic Cr(VI) from different environmental water samples such as double-distilled water (DDW), tab water, synthetic seawater, natural seawater, and real wastewater obtained from Teraat Al Esmaieliah and Bahr El-Baqar drain. The adsorption ability of PGP-1N H_2SO_4 for Cr(VI) removal from aqueous solution was studied at different pH, contact time, initial concentrations of adsorbate, sorbent mass, and temperature. The kinetics, isotherms, and thermodynamics for the sorption of Cr(VI) on the prepared samples were studied.

2. Experimental setup

2.1. Biosorbent preparation

The pomegranate peel waste was washed with tap water, dried in sunlight until the moisture was partially evaporated, and was further washed by DDW then dried in a hot air oven at 80°C ± 2°C for 1 d. This dried material was crushed into small granules and divided into five parts, each part weighted 20 g. The first part was soaked with DDW overnight and then filtered, this process was repeated several times until get rid of all colored or soluble materials, then filtered and dried in a hot air oven at 80°C ± 2°C for 2 d. The remaining four parts were boiled with 1 N (NaOH, HNO_3, H_2SO_4, and HCl) solution respectively, in a ratio of pomegranate peel to treatment solution 1:10 w/v and kept to cool at room temperature overnight. Thereafter, each part was washed with DDW several times to remove the excess treatment solution if any, until the pH of the suspension reached ~4.75, then filtered and dried in a hot air oven at 80°C ± 2°C for 2 d. All the dried materials were ground well-using a ball mill and sieved to obtain particle sizes in the range of 168–212 μm. The product is preserved in airtight vessel for further studies.

2.2. Preparation of synthetic solution and analysis

All the chemicals used in this work were of an analytical grade and used as purchased without additional purification. Except for the reaction temperature parameter, all the adsorption experiments were carried out at room temperature 25°C ± 1°C. A stock solution of Cr(VI) (1,000 mg/L) was obtained by dissolving 2.8288 g of $K_2Cr_2O_7$ in 1,000 mL of DDW and then was used for further experimental solution preparation. Before mixing the adsorbent and chromium solution, the initial pH of each test solution was adjusted to the required value with 0.1 M HCl or 0.1 M NaOH, pH measurements were done using a pH meter of model 601A (USA). The concentration of free Cr(VI) ions in the stock solutions and unadsorbed Cr(VI) in the reaction medium was determined using inductively coupled plasma spectrophotometer (ICPs-7500, Shimadzu, Kyoto, Japan).

2.3. Simulation studies

About 75 mg/L from Cr(VI) ions were prepared in different water samples by dissolving about 0.021216 g of $K_2Cr_2O_7$ in 100 mL of the desired water sample. These water samples include DDW, tab water, synthetic seawater, natural seawater, and real wastewater obtained from Teraat Al Esmaieliah and Bahr El-Baqar drain. The synthetic seawater was obtained by dissolving 3.5 g of NaCl in 100 mL DDW. The natural seawater was obtained from coastal water (salinity 37 ± 1 g/L). The filtered wastewater, which was collected from Teraat Al Esmaieliah (Egypt) contains several industrial effluents and agriculture drain. The filtered sewage was collected from the Bahr El-Baqar drain (in northeastern Egypt). The pH of the desired water sample was adjusted to be 3.0 using 0.1 M HCl.

2.4. Activated carbon selection

The five-carbon samples understudies were evaluated for their specific ability to remove Cr(VI) from aqueous solutions. These experiments were done at the original pH of the solutions. In this concern, 0.1 g of each carbon was conducted with 25 mL of 75 mg/L of Cr(VI) solutions using a thermostatic shaker water bath (Kottermann D-1362, Germany) at 25°C ± 1°C for 24 h. The solutions were filtered. The amount of Cr(VI) sorbed on the selected carbon sample was evaluated and the sample which gave the maximum uptake was selected and utilized for the remaining experiments. To correct for any adsorption of Cr(VI) on containers, control experiments were done without adsorbent. There is no adsorption by the container wall.

2.5. Characterization of selected biosorbent material

The particle diameter of the prepared PGP-1N H_2SO_4 was determined using a sieving technique with different mesh sizes ranging from 100 to 1,000 μm using RP 200N Model, Spain, UE. Some physical and chemical properties of the PGP-1N H_2SO_4 such as apparent and packed densities, ash, and moisture contents were studied using the techniques presented in the previously reported work (for a sake of brevity) [27].

FT-IR (BOMEM-FTIR Model, Shimadzu, Kyoto, Japan) for the prepared samples was done to investigate their surface functional groups; the condition of the experiment was adjusted in the wavenumber range of 400–4,000 cm⁻¹. The FT-IR spectra of the prepared adsorbent were achieved using the KBr disc method. The solid PGP-1N H_2SO_4 sample was mixed with KBr in a ratio of 1:5 and ground to a very fine powder. A transparent disc was formed in a moisture-free atmosphere. SEM (Jeol SEM of JSM-6510A model, Japan, operating with beams of primary electrons ranging from 5 to 30 keV) was used to identify the morphological structure of the chemically activated pomegranate peel samples. TGA was completed using a Shimadzu thermal analyzer obtained from Shimadzu (Kyoto, Japan). PGP-1N H_2SO_4 sample was heated from room temperature up to 1,000°C in the N_2 atmosphere with a heating rate of 20°/min and using alumina powder as reference material. XRD analysis (XD–Dl model, Shimadzu, Kyoto, Japan) was employed to identify any

crystallographic structure in the adsorbents. The operating conditions were 30 kV and 30 mA and a diffraction angle (2θ) range of 4°–90°. A nickel filter and Cu K_α-X-ray tube ($\lambda = 1.5418$ Å) were used.

2.6. Batch adsorption studies

2.6.1. Effect of pH (Optimum pH determination)

To know the optimum solution pH at which the maximum adsorption of Cr(VI) was achieved, the initial pH values were adjusted to 1.0, 1.5, 2.0, 2.5, 3.0, 3.5, 4.0, 5.0, and 6.0 using 0.1 M HCl or 0.1 M NaOH solutions. 0.1 g of adsorbent was contacted with 25 mL of Cr(VI) solution of 75 mg/L at 25°C ± 1°C in a thermostatic water bath shaker (Kottermann D-1362, Germany) at a constant agitation speed of 250 rpm for the minimum contact time required to reach the equilibrium (180 min). The solution pH for maximum metal adsorption was then selected and utilized for the remaining experiments.

2.6.2. Effect of biosorbent mass

The effect of sorbent mass on the sorption of Cr(VI) was studied by mixing 25 mL solution containing 75 mg/L of Cr(VI) ions with different PGP-1N H_2SO_4 mass (0.03, 0.05, 0.08, 0.1, 0.2, 0.4, and 0.6 g) for respective equilibrium times (180 min) at 25°C ± 1°C and optimum pH value of 3.0. The solution was filtered and the chromium concentration was determined.

2.6.3. Effect of temperature

The influence of temperature on the sorption of Cr(VI) was determined by using five different temperatures (i.e., 298, 308, 318, 328, and 338 K). 0.1 g of the sorbent was transferred into conical flasks containing 25 mL of 100 mg/L Cr(VI) ions, the conical flasks were shaken in a thermostatic water bath shaker at a constant agitation speed of 250 rpm for 180 min.

2.6.4. Kinetics studies

Kinetic studies were achieved by shaking 0.1 g of PGP-1N H_2SO_4 adsorbent with 25 mL Cr(VI) solution (75 mg/L) at 25°C ± 1°C and an optimum pH value of 3.0 in a thermostatic water bath shaker (Kottermann D-1362, Germany) at a constant agitation speed of 250 rpm. The residual Cr(VI) concentration was measured after fixed time period (15, 30, 45, 60, 75, 90, 120, 150, 180, and 240 min).

2.6.5. Adsorption isotherm

Adsorption isotherm experiments were carried out in 100 mL conical flasks at 25°C ± 1°C on a shaker for 180 min. 0.1 g of PGP-1N H_2SO_4 sample was completely mixed with 25 mL of Cr(VI) solutions. The isotherm studies were done by varying the initial Cr(VI) concentrations from 20 to 400 mg/L at pH 3.0. After shaking the flasks for 180 min, the mixture was filtered and the residual Cr(VI) concentration in the separated solution was measured using ICPs-7500. All the

experiments are repeated three times and then the average for the values are assigned. The total experimental percentage error did not exceed 3%. The removal percentage and amount of Cr(VI) adsorbed onto PGP-1N H_2SO_4 adsorbent at equilibrium, q_e (mg/g) were calculated using Eqs. (1) and (2), respectively:

$$Removal\ (\%) = \left(\frac{C_0 - C_e}{C_0}\right) \times 100 \tag{1}$$

$$q_e\ (mg/g) = \frac{(C_0 - C_e)V}{m} \tag{2}$$

where C_0 and C_e (mg/L) are the initial and equilibrium concentrations of Cr(VI) ions, respectively. V is the volume of the solution (L), and m is the mass of dry adsorbent used (g).

3. Results and discussion

3.1. Activated carbon selection

To select the best carbon sample appropriate for the retention of Cr(VI) ions from wastewater streams, Table 1 illustrates the results obtained for the scavenging of Cr(VI) ions from the polluted water using unmodified and chemically modified pomegranate peel. There is an obvious difference in the efficiency of the five-carbon samples to uptake Cr(VI) ions from polluted water. This significant difference in the amount of Cr(VI) ions adsorbed on the tested samples indicates different interaction mechanisms between chromium ions and carbon surface. As shown from Table 1, the sample treated with H_2SO_4 is found to be superior in the scavenging of Cr(VI) ions from polluted solution, so this sample was selected for further investigations. The detailed characteristics of PGP-1N H_2SO_4 obtained are given in Table 2. It was granular in nature, exhibited considerable apparent and bulk density, resistant to HNO_3 and HCl media, and showed high Cr(VI) removal, therefore it was chosen for detailed study.

3.2. Characterization

3.2.1. Scanning electron microscopy

The surface physical morphology of raw pomegranate peel (untreated-PGP), chemically modified pomegranate peel (PGP-1N HNO_3, PGP-1N HCl, PGP-1N NaOH, and PGP-1N H_2SO_4), and Cr-sorbed PGP-1N H_2SO_4 samples

were observed by SEM as shown in Fig. 1. The SEM micrographs of untreated pomegranate peels (Fig. 1a), PGP-1N HNO_3 (Fig. 1b), and PGP-1N NaOH (Fig. 1d) are similar in appearance were showed that the fibers are stuck together due to the existence of crude fibers, protein, lignin, and other viscous compounds [2]. The surface morphology of untreated-PGP wasn't affected by modification with HNO_3 and NaOH, and this is the main reason that their efficiencies for Cr(VI) removal are low compared to PGP-1N HCl and PGP-1N H_2SO_4. The chemically modified pomegranate peels PGP-1N HCl (Fig. 1c) and PGP-1N H_2SO_4 (Fig. 1e(1)), show extensive external surface with extremely irregular cavities and pores. These pores and cavities result from the evaporation of chemical reagent (HCl or H_2SO_4) during activation leaving the space open that was previously occupied by HCl or H_2SO_4 [17,45], in addition to, the viscous compounds are removed during chemical treatment [2]. This noticeable change in appearance after the modification with HCl and H_2SO_4 is the main reason for increasing the chromium removal efficiency. As it is obvious from Fig. 1e(2) that an obvious change in the surface of the PGP-1N H_2SO_4 after Cr(VI) adsorption has been noticed, the surface morphology of the adsorbent became much smoother after the adsorption of Cr(VI), and the pores and cavities are filled by Cr(VI) ions.

3.2.2. FT-IR analysis

The functional groups onto the surface of selected activated pomegranate peel samples (PGP-1N H_2SO_4) were analyzed by FT-IR. The FT-IR bands of PGP-1N H_2SO_4 and Cr-sorbed PGP-1N H_2SO_4 are given in Fig. 2. Abroad peak at 3,425 cm^{-1} represents the –OH stretching vibrations of cellulose and lignin [46,47]. Bands at 2,924 and 2,853 cm^{-1} are mainly due to asymmetric vibration mode and symmetric stretching of CH and indicative of the presence of aliphatic –CH_2 groups [48]. There was an obvious band at 1,717 cm^{-1}, which may be characteristic of stretching mode of C=O in acetyl or ester groups of hemicelluloses and ester linkage in lignin [49,50]. The band at 1,618 cm^{-1} corresponds to the

Table 1
Preliminary tests for untreated and chemically modified pomegranate peel

Adsorbent	q_e (mg/g)
Untreated-PGP	7.46
PGP-1N NaOH	0.05
PGP-1N HCl	15.04
PGP-1N HNO_3	4.21
PGP-1N H_2SO_4	18.00

Table 2
Characteristics of chemically activated pomegranate peel (PGP-1N H_2SO_4)

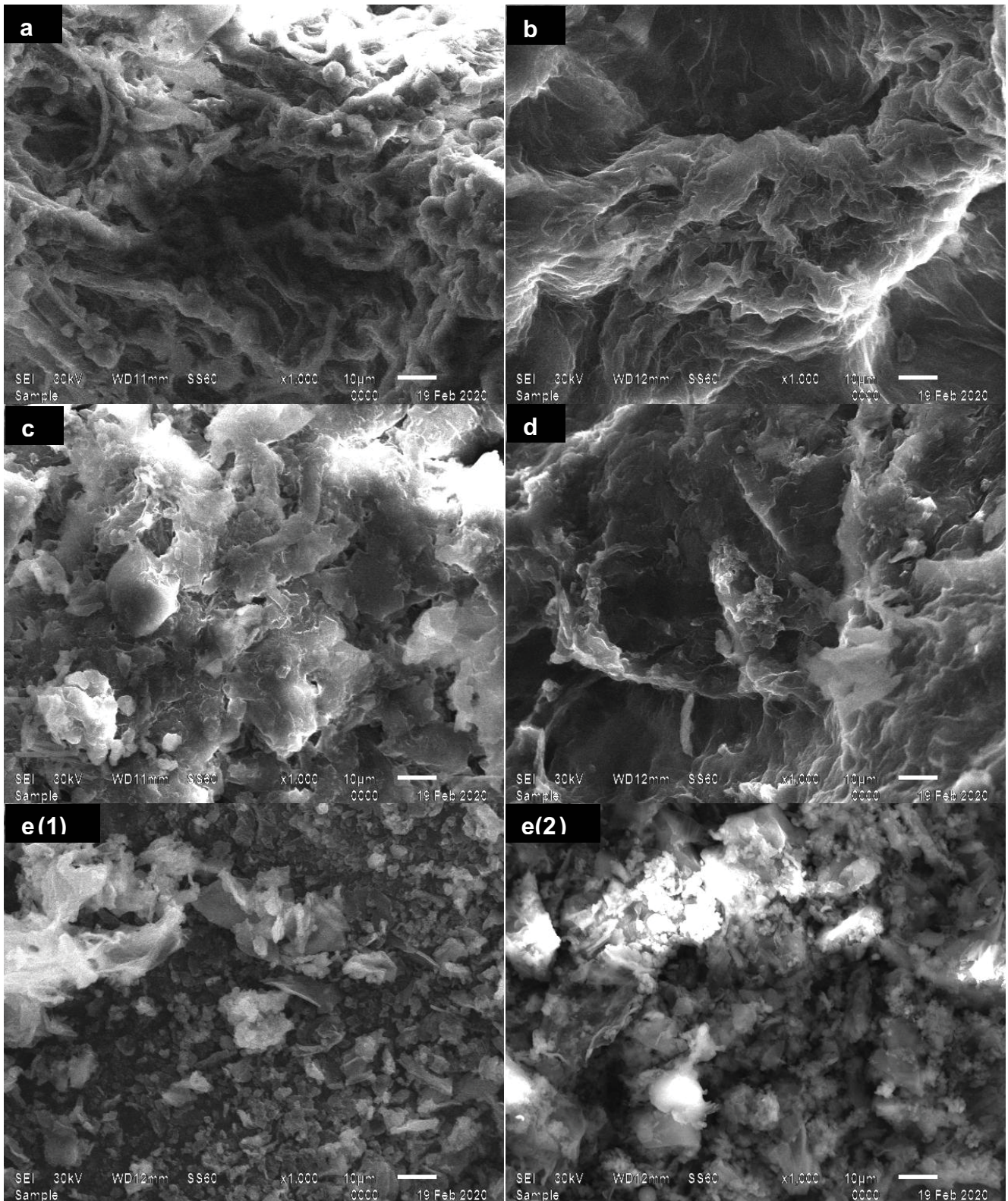| Characteristics	Values
Moisture content (%)	11.40
Ash content (%)	6.56
Bulk density (g/mL)	0.420
Apparent density (g/mL)	0.305
Average particle size (μm)	168–212
Yield %	35
pH	4.75
Adsorption capacity (mg/g)	18.0
Solubility in water (%)	0.075
Solubility in 0.5 M HCl (%)	0.30
Solubility in 5 M HCl (%)	1.20
Solubility in 0.5 M HNO_3 (%)	0.35
Solubility in 5 M HNO_3 (%)	1.45

Fig. 1. SEM micrographs of (a) untreated-PGP, (b) PGP-1N HNO_3, (c) PGP-1N HCl, (d) PGP-1N NaOH, (e) [(1) PGP-1N H_2SO_4 and (2) Cr-sorbed PGP-1N H_2SO_4] magnitude of 1,000×.
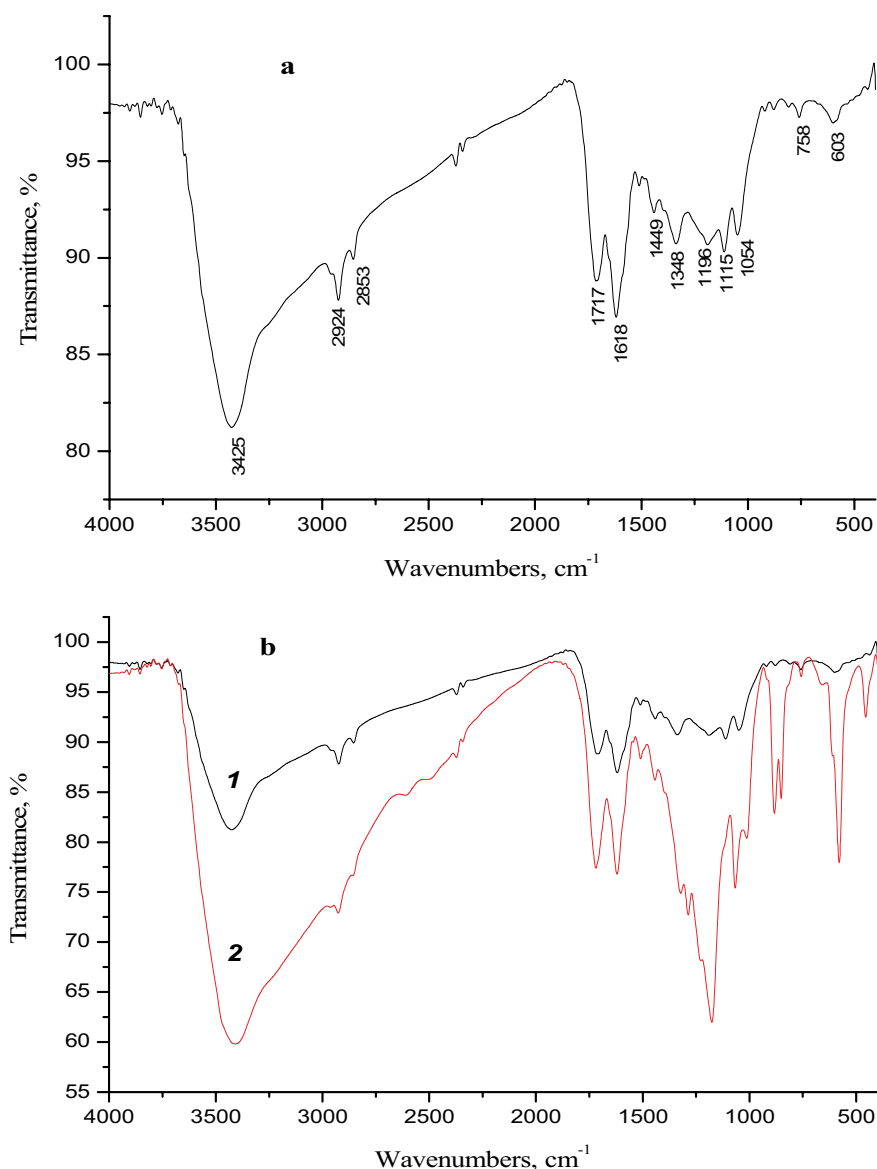
Fig. 2. FT-IR spectrum of (a) PGP-1N H$_2$SO$_4$ sample and (b) [(1) unloaded PGP-1N H$_2$SO$_4$ and (2) Cr-sorbed PGP-1N H$_2$SO$_4$].

bending vibrations of adsorbed water [51]. The peaks at 1,450 and 1,115 cm^{-1} are ascribed with the C–O stretching [12,51,52]. The absorbance band near 1,348 cm^{-1} was related to –CH symmetric bending vibrations [53]. The peaks at 1,196 and 1,054 cm^{-1} correspond to the non-symmetrical C–O–C and C–OH vibrations of cellulose, respectively [54]. The bands between 603 and 758 cm^{-1} are associated with metal–oxygen bonds [51]. After Cr(VI) adsorption, a slight shifting of the band from 3,425 to 3,415 cm^{-1} has been occurring and it proves the electrostatic interaction between Cr(VI) ions and PGP-1N H$_2$SO$_4$ biosorbent material. The new band at 456 cm^{-1} in the Cr-sorbed PGP-1N H$_2$SO$_4$ could be due to the formation of Cr(OH)$_3$ which suggests the reduction of Cr(VI) to Cr(III) [55,56]. The obtained results confirm that the –OH group of cellulose and lignin was involved in the adsorption of Cr(VI).

3.2.3. Thermogravimetric analysis

The TGA curve of the PGP-1N H$_2$SO$_4$ sample is presented in Fig. 3. Regarding the TGA curve, observe that as the sample heated from room temperature up to 1,000°C. PGP–1N H$_2$SO$_4$ sample exhibits a significant weight loss of about 11.4% when the sample heated from room temperature to 180°C attributed to the evaporation of the coordinated or adsorbed water [29]. At the temperature range of 180°C–332°C, the percent weight loss gradually increases until reaches to 29.8% and this may be due to the loss of an organic part of the PGP–1N H$_2$SO$_4$ adsorbent [29]. Further increase in temperature causes the percentage of weight loss to increase, at the temperature range of 332°C to 850°C, the weight loss of about 52.30% was observed. Such weight loss is probably attributed to the loss of the more stable organic part of PGP–1N H$_2$SO$_4$ [29].
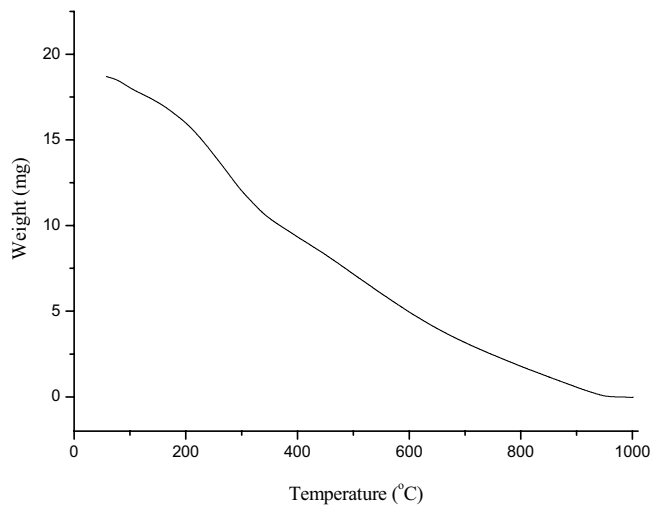
Fig. 3. TGA curve of PGP-1N H$_2$SO$_4$.

Fig. 4. XRD pattern of PGP-1N H$_2$SO$_4$.

3.2.4. XRD analysis

The XRD analysis was carried out to know the crystal structure of the PGP-1N H$_2$SO$_4$ as well as to use in qualitative analysis through knowing the corresponding component at each spectrum. The spectrum of the PGP-1N H$_2$SO$_4$ sample is presented in Fig. 4. The diffraction pattern for PGP-1N H$_2$SO$_4$ shows an intense peak at 2θ = 16.96°, 22.34°, and 27.72° are the characteristic peaks of cellulose fibers, which coincides with reported literature values [28,54,57,58].

3.3. Adsorption studies

3.3.1. Effect of contact time

Fig. 5a shows that the sorption of Cr(VI) by PGP-1N H$_2$SO$_4$ was affected by the variation of contact time. At the starting, the rate of adsorption reaction is so rapid, about 50% of Cr(VI) was retained on the adsorbent surface at first 15 min, and thereafter the rate of adsorption of Cr(VI) onto activated pomegranate peel found to be slow, repulsion force, or electrostatic hindrance which initiate between pomegranate peel surface loaded with negative chromium ions and the anionic Cr(VI) available in solution may responsible for slows down of the reaction, as well as the slow pore diffusion of the Cr(VI) ion into the bulk of adsorbent [31]. The removal percentage and amount of Cr(VI) ions adsorbed by PGP-1N H$_2$SO$_4$ (q_e) have become constant about 96% and 18 mg/g respectively, at 3 h. Therefore the time at which the equilibrium is achieved is 3 h and all experiments have been performed.

3.3.2. Effect of pH

The solution pH mainly affects the surface charge, the degree of ionization, and the adsorbates species [51,59]. Fig. 5b shows the extent of removal of Cr(VI) as a function of pH for an initial concentration of 75 mg/L using the PGP-1N H$_2$SO$_4$ sample. It was noticed that the maximum removal percentage (96%) was attained at pH 3.0. The predominant species of chromium ions in the acidic medium are $Cr_2O_7^{-2}$,
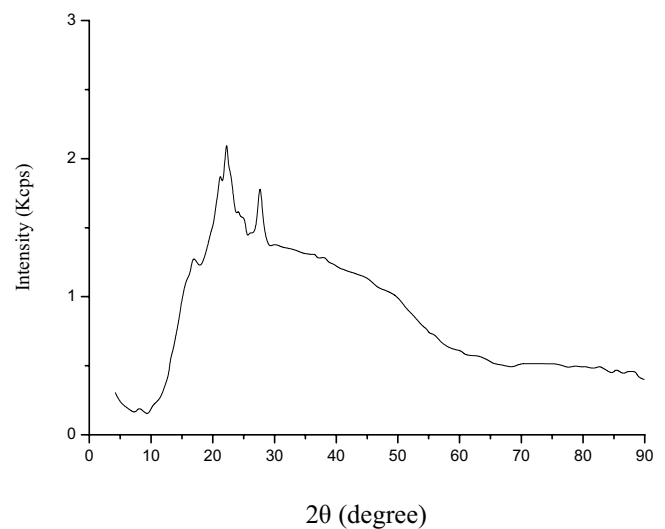
$HCrO_4^-$, $Cr_3O_{10}^{-2}$, and $Cr_4O_{13}^{-2}$ [2,38]. At low pH, the adsorbent surface becomes highly protonated, so the adsorption of anionic Cr(VI) ions on the protonated adsorbent surface is enhanced. The protonation of the adsorbent surface is reduced with increasing the pH value which causes the electrostatic attraction between PGP-1N H$_2$SO$_4$ surface and anionic Cr(VI) is reduced, then the sorption of Cr(VI) ions by PGP-1N H$_2$SO$_4$ sample is decreased [2,38]. Besides, the competition occurred between OH$^-$ and chromate ions, CrO_4^{-2} when the pH value increases, and alkaline properties predominated. The mechanism of Cr(VI) adsorption on the surface of PGP-1N H$_2$SO$_4$ is illustrated in Fig. 6.

3.3.3. Effect of initial metal ion concentration

The retention of Cr(VI) by PGP-1N H$_2$SO$_4$ was studied by varying initial Cr(VI) concentration from 20 to 400 mg/L using optimum PGP-1N H$_2$SO$_4$ mass (0.1 g), temperature (25°C ± 1°C) for a contact time of 180 min (Fig. 5c). It was found that the % removal of Cr(VI) was decreased from 97.0% to 28.3% when the concentration of Cr(VI) was increased from 20 to 400 mg/L, which may be due to the less availability of adsorption sites at a higher dose of Cr(VI) ions [60].

3.3.4. Effect of biosorbent mass

Studying the effect of the sorbent mass on the removal of Cr(VI) ions was carried out by varying the adsorbent quantity from 0.03 to 0.6 g in solution while considering the other operational parameters be constant (initial chromium concentration, 75 mg/L; temperature, 298 K; pH, 3.0; time, 3 h.). The values of % removal and q_e at a different mass of PGP-1N H$_2$SO$_4$ were presented in Fig. 5d. The % removal of Cr(VI) ions increased from 38.32% to 96.65% with increasing the biosorbent mass from 0.03 to 0.6 g, respectively. This is a result of more available binding sites when the mass of biosorbent increased [2,5,38,56,61]. However, the values q_e (mg/g), was reduced from 23.95 to 3.02 mg/g with increasing biosorbent mass. This caused by the existence of
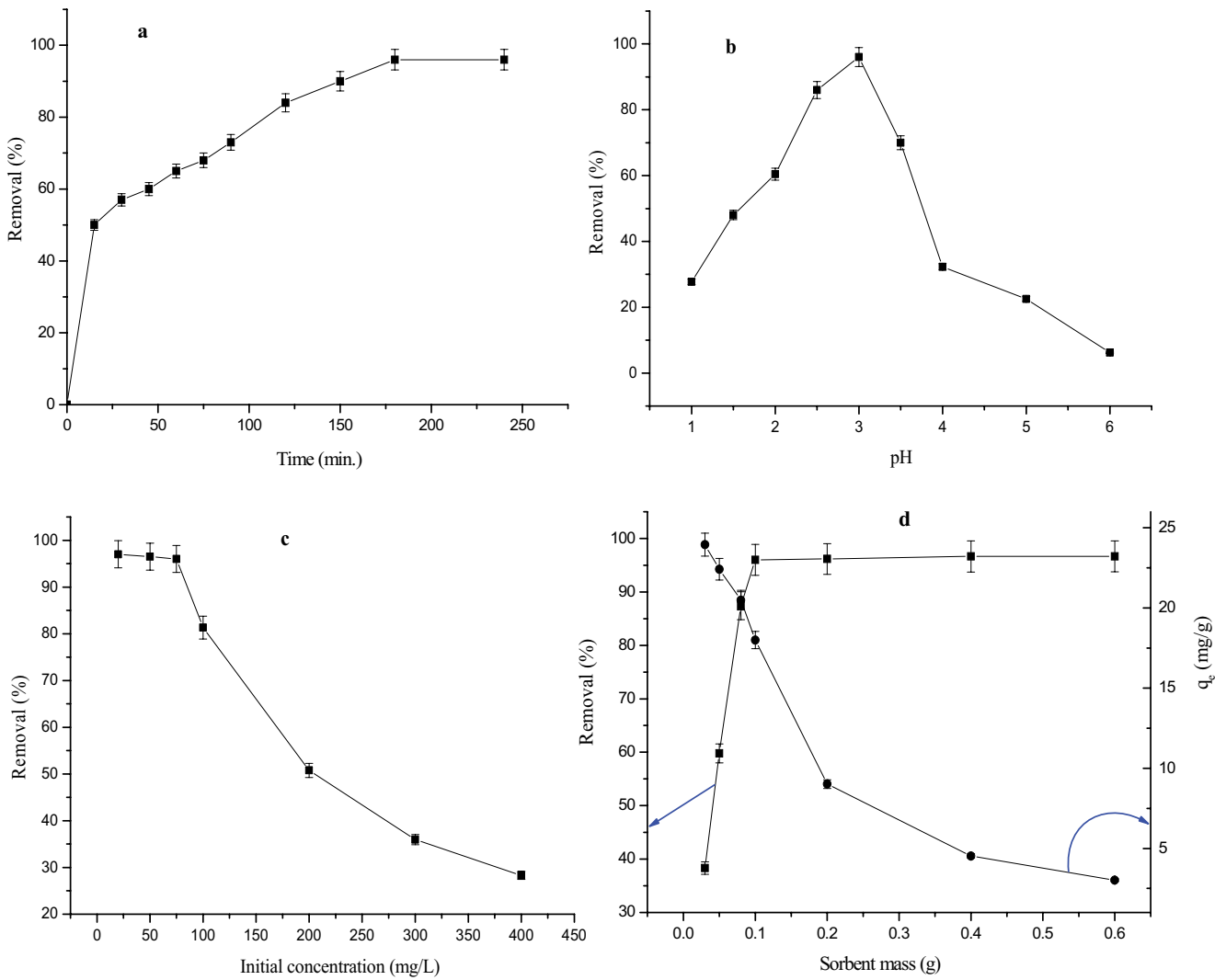
Fig. 5. Effect of some operational parameters on the removal of Cr(VI) by PGP-1N H$_2$SO$_4$ (a) time, (b) pH, (c) initial concentration, and (d) sorbent mass.
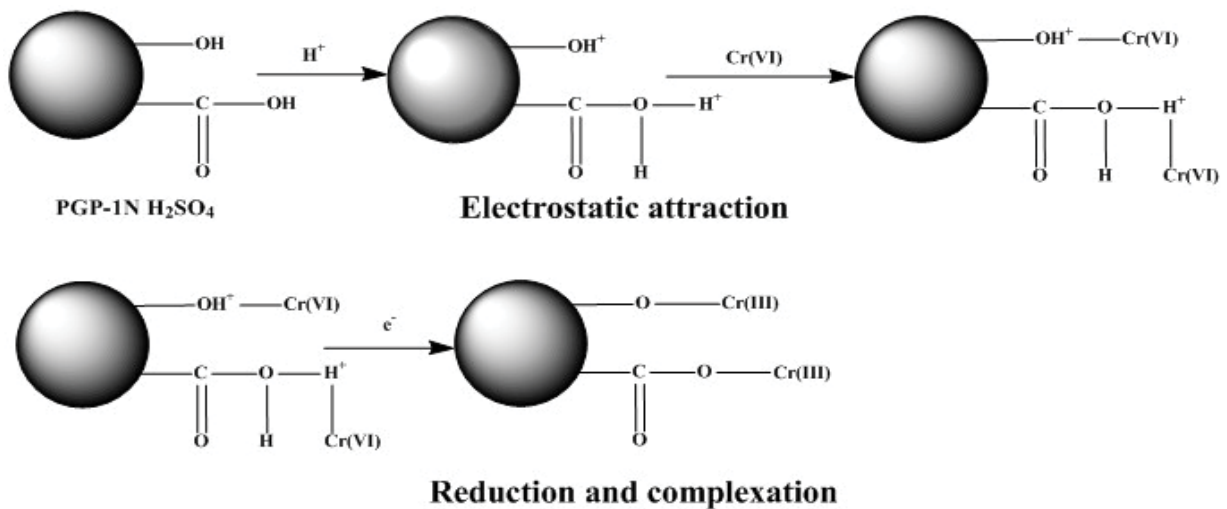

Fig. 6. Proposed removal mechanism of Cr(VI) by PGP-1N H$_2$SO$_4$.

a high number of vacant available sites during biosorption process. Comparable results were previously obtained by other researchers [62,63].

3.4. Adsorption kinetic studies

Discussing the kinetic modeling for the adsorption process leads to understanding the dynamics of the adsorption reaction as well as the order of the rate constant. Batch experiments were done to investigate the rate of Cr(VI) adsorbed by PGP-1N H_2SO_4. It is very important to study the mechanism of the reaction and the mechanism of diffusion to examine the rate-controlling steps of the adsorption process.

3.4.1. Mechanism of the reaction

To achieve the mechanism of adsorption, three different kinetic models (pseudo-first-order, pseudo-second-order, and Elovich) were applied and illustrated as follows:

The pseudo-first-order model [64]:

$$\log\left(q_e - q_t\right) = \log q_e - \frac{k_1}{2.303}t \tag{3}$$

The pseudo-second-order model [65,66]:

$$\frac{t}{q_t} = \frac{t}{q_e} + \frac{1}{k_2 q_e^2} \tag{4}$$

The Elovich model [67]:

$$q_t = \frac{1}{\beta}\ln(\alpha\beta) + \frac{1}{\beta}\ln(t) \tag{5}$$

where q_e and q_t are the amounts of Cr(VI) adsorbed at equilibrium and at any time t, respectively, in mg/g, k_1 (1/min) and k_2 (g/mg min) are the pseudo-first-order and pseudo-second-order rate constant, respectively, α (mg/g/min), and β (g/mg) are the Elovich constants. The results of the above three kinetics models are given in Table 3. The correlation coefficient values were much higher for the pseudo-second-order ($R^2 > 0.992$) (Fig. 7b) than the pseudo-first-order ($R^2 > 0.968$) (Fig. 7a) and Elovich ($R^2 > 0.963$) (Fig. 7c) kinetics model. In addition to the calculated q_e value obtained from pseudo-second-order rate expression (20.44) are closely agrees with the experimental data (18.00). These results proposed that experimental data are applicable well with the pseudo-second-order model. So a chemical interaction occurred between functional groups on the adsorbent surface and Cr(VI) ions, then the rate-determining step of the reaction is the chemisorption of Cr(VI) ions in the adsorption process [68].

3.4.2. Mechanism of the diffusion

The diffusion of the adsorbate on the adsorbent surface can be controlled by three steps viz. film diffusion, pore diffusion, and intra-particle transport. The slowest of the three steps controls the overall rate of the process. Generally, pore diffusion and intra-particle diffusion are often rate-limiting in a batch reactor, which for continuous flow system film diffusion is more probably the rate-limiting step [69]. The intra-particle diffusion model can be investigated in its linear shape using the next equation [70]:

$$q_t = k_{id}t^{0.5} + C \tag{6}$$

The intra-particle diffusion rates (k_{id}) and the constant (C) were evaluated from the graphing of q_t vs. $t^{0.5}$ as illustrated in Fig. 7d. If intra-particle diffusion is a rate-controlling step, then the plot should be linear and pass through the origin, which is not the case in this study. The deviation of straight lines from the origin, as shown in Fig. 7d, suggesting the involvement of intra-particle diffusion in the adsorption process but not as the rate-controlling step, other kinetic models along with the intra-particle diffusion may dominate the rate of adsorption, which can be operating concurrently [71].

3.5. Adsorption isotherm investigation

The experimental data were analyzed using different isotherm models such as Langmuir, Freundlich, Temkin, and Dubinin–Radushkevich (D–R) isotherm models, and the constant parameters of the isotherm equations were estimated and summarized in Table 4. For each isotherm, various concentrations of Cr(VI) ions solution were mixed with a fixed adsorbent weight in each sample. Fig. 8 shows the adsorption isotherm of Cr(VI) onto the PGP-1N H_2SO_4 sample.

3.5.1. Langmuir isotherm

The Langmuir equation assumed the validity of a homogeneous monolayer surface with a finite number of identical sites for the adsorption process. The interaction between adsorbed molecules is negligible; the linear form is presented as following [72]:

Table 3
Parameters of different estimated kinetics models for the adsorption of Cr(VI) onto PGP-1N H_2SO_4

Model	Parameter	Value
Pseudo-first-order kinetic model	k_1 (min^{-1})	0.015
	$q_{e,cal}$ (mg/g)	12.81
	R^2	0.96861
Pseudo-second-order kinetic model	k_2 (g/mg min)	0.00145
	$q_{e,cal}$ (mg/g)	20.44
	R^2	0.99257
Elovich equation	α (mg/g min)	0.864
	β (g/mg)	0.284
	R^2	0.96399
Intraparticle diffusion	k_{id} (mg/g min$^{1/2}$)	0.925
	C	5.316
	R^2	0.99127
Practical capacity	$q_{e,exp}$ (mg/g)	18.00

$$\frac{C_e}{q_e} = \frac{C_e}{q_{max}} + \frac{1}{bq_{max}} \tag{7}$$

where C_e is the equilibrium concentration in solution (mg/L), q_e is the amount of metal ion adsorbed at equilibrium (mg/g), q_{max} is the maximum monolayer capacity of the adsorbent (mg/g), and b is Langmuir equilibrium constant (L/mg) that related to the apparent energy of sorption. Eq. (7) is the most popular linear form of the Langmuir isotherm model. The values of q_{max} and b constants and correlation coefficients for Langmuir isotherm were evaluated from the plot of C_e/q_e vs. C_e (Fig. 8a) and presented in Table 4. The correlation coefficient (R^2) for the adsorption of Cr(VI) onto the PGP-1N H_2SO_4 sample is higher than 0.999, and the theoretical values of q_{max} consistent well with the experimental values, which indicate that the Langmuir model is applicable.

The dimensionless constant separation term (R_L) was used to prove the applicability of the Langmuir isotherm model. The R_L value can be estimated using the following equation [73]:

$$R_L = \frac{1}{1 + bC_0} \tag{8}$$

where C_0 is the largest initial concentration of Cr(VI) ions in solution (400 mg/L). The R_L is greater than 0 but less than 1 suggesting that Langmuir isotherm is applicable [74]. Langmuir isotherm model is symmetrical to the experimental data which may be due to the homogeneous distribution of active sites on the PGP-1N H_2SO_4.

Table 5 summarizes the reported values of q_{max} in the literature using various adsorbents. PGP-1N H_2SO_4
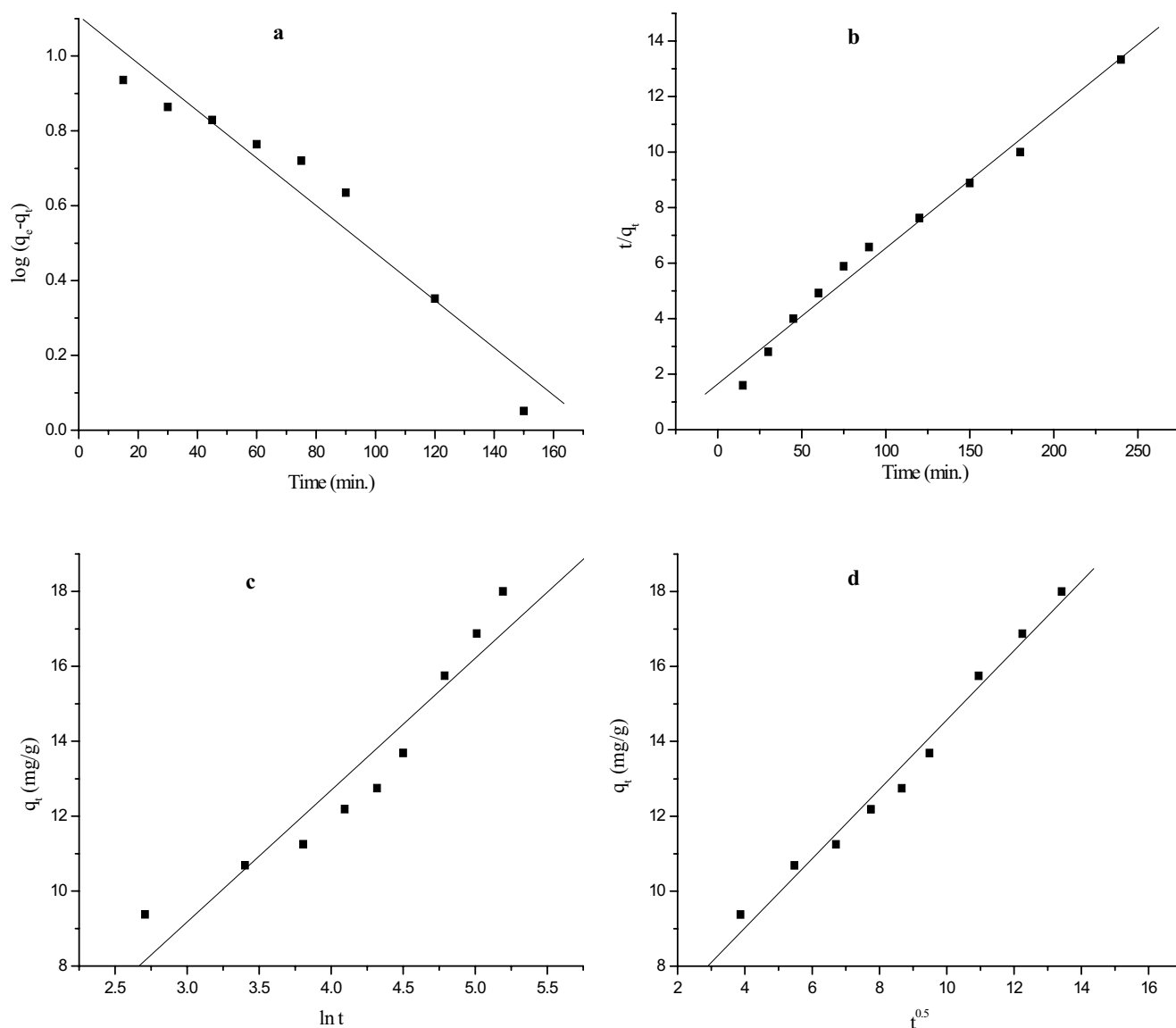

Fig. 7. Kinetics of Cr(VI) adsorption onto PGP-1N H_2SO_4 (a) pseudo-first-order model, (b) pseudo-second-order model, (c) Elovich model, and (d) intraparticle diffusion at initial Cr(VI) concentration 75 mg/L, pH = 3.0, and 25°C ± 1°C.

adsorbent gave good values of q_{max} compared with other adsorbents.

3.5.2. Freundlich isotherm

Freundlich isotherm suggested that the heterogeneous surface character of the sorbent material and the distribution of heat of sorption over that surface is non-uniform. The linear mathematical expression is formulated as follows [90]:

$$\log q_e = \log K_F + \frac{1}{n}\log C_e \tag{9}$$

where K_F (mg/g) and $1/n$ are Freundlich isotherm constants indicate the capacity and intensity of the adsorption, respectively. The values of K_F and $1/n$ were calculated from the linear plot of $\log q_e$ vs. $\log C_e$ (Fig. 8b) which are given in Table 4. It was found that the plots exhibit deviation from linearity at the concentration range (>75 mg/L). However, the correlation coefficients in Table 4 indicate the data are not well-correlated to Freundlich correlation coefficients ($R^2 = 0.88117$) compared to the Langmuir correlation coefficients ($R^2 = 0.99928$). By comparing the results presented in Table 4, it is possible to conclude that the Langmuir sorption isotherm can accurately describe the adsorption of Cr(VI) onto PGP-1N H_2SO_4 in this study.

3.5.3. Temkin isotherm

The Temkin isotherm model describes the adsorbent species–adsorbate interactions. It postulates the following basics:
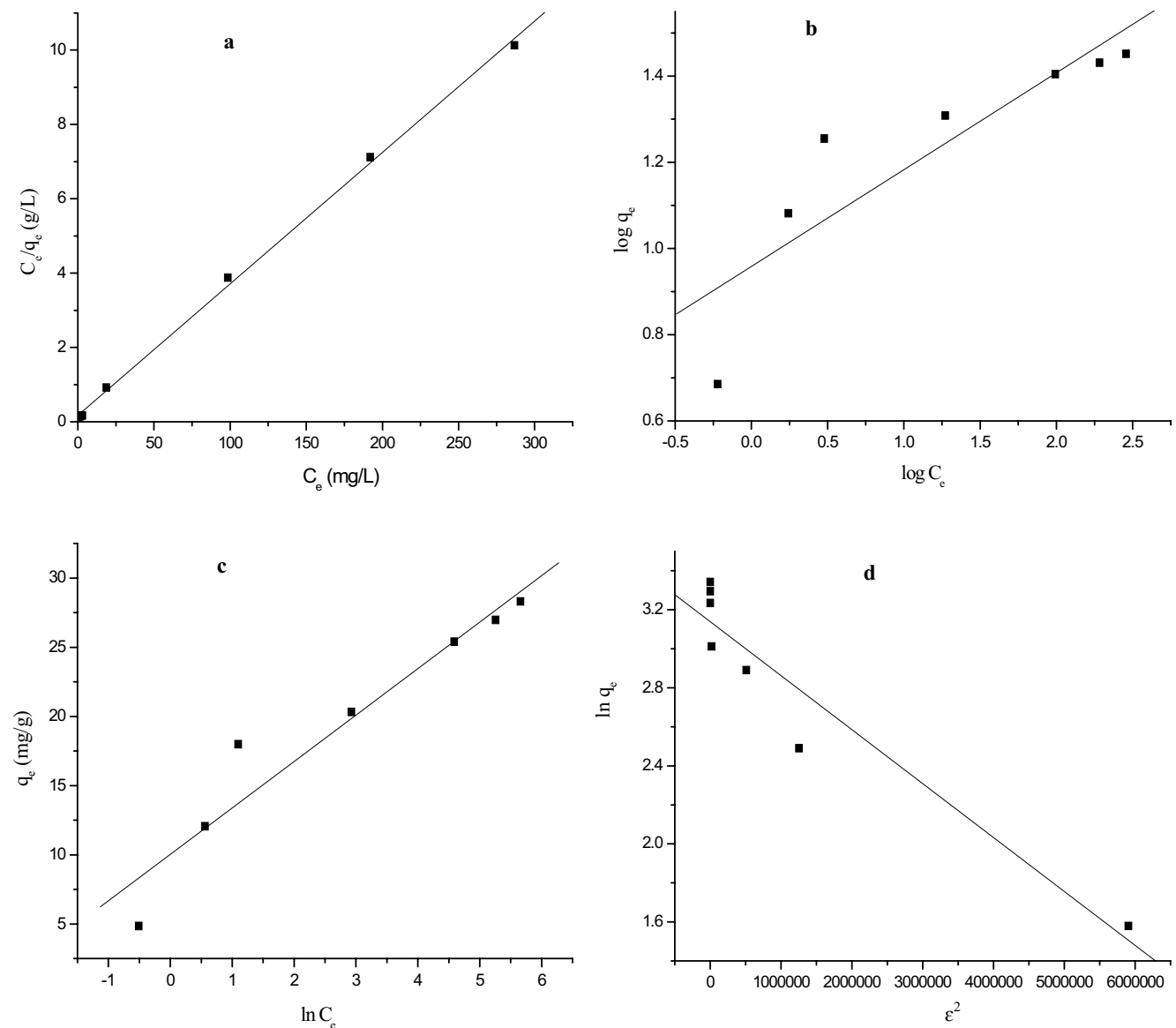

Fig. 8. Linearized form of (a) Langmuir, (b) Freundlich, (c) Temkin, and (d) Dubinin–Radushkevich isotherm models for the adsorption of Cr(VI) onto PGP-1N H_2SO_4 sample at 25°C ± 1°C.

- When the surface of the adsorbent is completely covered with adsorbate ions, this leads to adsorbate–adsorbate repulsions, accordingly the heat of adsorption of all the molecules in the layer decreases.
- The adsorption is a uniform distribution of maximum binding energy.
- The lowering in the heat of sorption is linear rather than logarithmic, as denoted in the Freundlich equation. It is commonly expressed in the next linear equation;

$$q_e = B \ln A_T + B \ln C_e \tag{10}$$

$$B = \frac{RT}{b} \tag{11}$$

where A_T is Temkin isotherm equilibrium binding constant (L/g), B is a constant corresponding to the heat of sorption (J/mol), T is the absolute temperature (K), and R is the universal gas constant, 8.314 J/mol/K. The linear plot of q_e vs. $\ln C_e$ for adsorption of Cr(VI) onto PGP-1N H$_2$SO$_4$ adsorbent is illustrated in Fig. 8c while, the Temkin constants for adsorbent are given in Table 4. The correlation coefficient ($R^2 = 0.96348$) was relatively high, which indicates the applicability of the Temkin equation. This could mean that the adsorption of Cr(VI) using PGP-1N H$_2$SO$_4$ adsorbent was a chemical adsorption process [91].

3.5.4. Dubinin–Radushkevich isotherm

Another equation employed in the explication of isotherms was submitted by Dubinin and Radushkevich (D–R) isotherm [92]. The linear form of the D–R isotherm equation can be expressed using the next equation:

Table 4
Langmuir, Freundlich, Temkin, and Dubinin–Radushkevich parameters for the sorption of Cr(VI) onto PGP-1N H$_2$SO$_4$

Model	Parameter	Value
Langmuir	q_{max} (mg/g)	28.28
	b (L/mg)	0.203
	R^2	0.99928
	R_L	0.012
Frendlich	K_F (mg/g)	9.08
	$1/n$	0.225
	R^2	0.88117
Temkin	A_T (L/g)	19.79
	B_T (J/mol)	3.36
	b	737.94
	R^2	0.96348
Dubinin–Radushkevich	q_m (mg/g)	23.06
	K_{D-R} (mol^2/kJ^2)	2.765×10^{-7}
	E (kJ/mol)	30.07
	R^2	0.95707
Experimental capacity	$q_{e,exp}$ (mg/g)	28.30

Table 5
Comparison of the maximum Cr(VI) adsorption capacity of various adsorbents

Adsorbent	Maximum adsorption capacity, q_{max} (mg/g)	References
Red mud	75.00	[1]
Grafted banana peels (GBPs)	6.17	[2]
Besicular basalt (VB)	104.0	[3]
CN-cl-PL(AA)NHG	26.49	[5]
Unoxidized carbon	13.68	[17]
Oxidized carbon	16.26	[17]
PANI/SiO$_2$ composite	63.41	[56]
β-CCWB450	124.42	[68]
Polypyrrole-polyaniline nanofibers	227.27	[75]
Sugar beet tailing biochar	123.00	[76]
FAC	21.75	[77]
SAC	9.535	[77]
ATFAC	9.866	[77]
ATSAC	11.51	[77]
ACF	96.30	[77]
Sago waste activated carbon	5.78	[78]
Clarified sludge	26.31	[79]
Rice husk ash	25.64	[79]
Activated alumina	25.57	[79]
Fuller's earth	23.58	[79]
Fly ash	23.86	[79]
Saw dust	20.70	[79]
Neem bark	19.60	[79]
Almond	10.62	[80]
Coal	6.78	[80]
Pine needles	21.50	[80]
Cactus	7.082	[80]
Tyres activated carbon (TAC)	48.08	[81]
Fe(III)/Cr(III) hydroxide	1.38	[82]
Mango stone ash (MSA)	4.73	[83]
Orange peel powder (OPP)	6.01	[83]
Corn cob ash (CCA)	4.21	[83]
Cow dung ash (CDA)	5.75	[83]
Granulated activated carbon (GAC)	10.17	[83]
Wheat bran	0.942	[84]
Hazelnut shell	17.70	[85]
Maize cob	13.8	[86]
Sugar cane bagasse	13.4	[86]
Sugar beet pulp	17.2	[86]
Palm pressed-fibers	15.00	[87]
Waste tea	1.55	[88]
Walnut shell	1.33	[88]
Modified oak sawdust	1.7	[89]
PGP-1N H$_2$SO$_4$	28.28	Current work

$$\ln q_e = \ln q_m - K_{D-R}\varepsilon^2 \qquad (12)$$

where K_{D-R} is D–R constant (mol²/KJ²) and ε is a Polanyi potential (J/mol) which estimated by the next equation:

$$\varepsilon = RT\ln\left(1 + \frac{1}{C_e}\right) \qquad (13)$$

In general, this model is used to estimate the value of free energy (E) which was used to differentiate the physical and chemical adsorption of metal ions, the value of mean free energy (E) can be calculated using the following equation [93,94]:

$$E = \frac{1}{\sqrt{2K_{D-R}}} \qquad (14)$$

The slope and intercept acquired from the linear plot of $\ln q_e$ vs. ε^2 (Fig. 8d) are used to estimate the values of q_m and K_{D-R}, respectively. These values and the value of correlation coefficient (R^2) are given in Table 4. The correlation coefficient of D–R isotherm ($R^2 = 0.95707$) for adsorption of Cr(VI) onto PGP-1N H₂SO₄ adsorbent is lower than the correlation coefficient of Langmuir isotherm ($R^2 = 0.99928$) and the theoretical value of q_m is much lower than the experimental value and even lower than that value obtained from Langmuir isotherm. We suggest that D–R isotherm is less applicable for the adsorption of Cr(VI) onto the PGP-1N H₂SO₄ sample compared to the Langmuir isotherm model. The values of the mean adsorption energy were found to be in the range of a chemical adsorption reaction, that is, 16–40 kJ/mol [74].

3.6. Effect of temperature and thermodynamics

The batch adsorption method was used to see the effect of varying temperatures (298–338 K) on the removal of Cr(VI) by PGP-1N H₂SO₄. The experimental results are illustrated in Fig. 9a which showed that the sorption of Cr(VI) was increased with temperature which may be due to increasing the mobility of the adsorbate ions within the pores of the adsorbent as a result of decreasing solution viscosity, in addition to some internal bonds on the edge of the sorbent surface were broken resulting in the creation of new active sites available for adsorption, so the adsorption capacity improved [62]. The adsorption of Cr(VI) was 81% at 298 K (25°C ± 1°C) but it was reached up to 95% at 338 K (65°C ± 1°C) which showed that the endothermic

Table 6
Thermodynamic parameters for the adsorption of Cr(VI) ions onto PGP-1N H₂SO₄

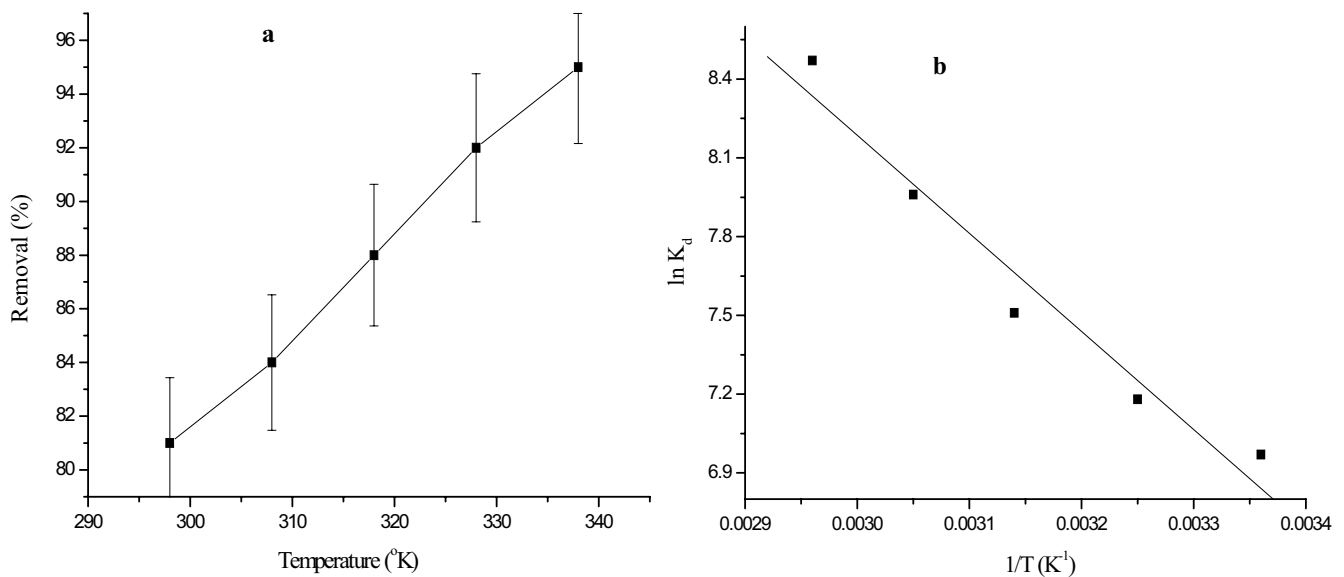| Sorbate	Temperature (K)	Removal, %	ΔH° (kJ/mol)	ΔS° (J/mol K)	ΔG° (kJ/mol)
	298	81.0			−17.27
	308	84.0			−18.39
Cr(VI)	318	88.0	31.08	161.29	−19.86
	328	92.0			−21.71
	338	95.0			−23.80

Fig. 9. Effect of reaction temperature on (a) removal (%) and (b) Van't Hoff plots for the removal of Cr(VI) by using PGP-1N H₂SO₄ at an agitating rate, 250 rpm; initial metal concentration, 100 mg/L; contact time, 180 min; volume, 25 mL; weight, 0.1 g; pH, 3.

nature of the adsorption process [95]. The dependence of temperature on the adsorption process is connected with several thermodynamic parameters viz. $\Delta G°$ (standard free energy change), $\Delta H°$ (standard enthalpy change), and $\Delta S°$ (standard entropy change). The values of $\Delta H°$ and $\Delta S°$ were calculated from the slopes and intercepts of the plots of $\ln K_d$ vs. $1/T$ (Fig. 9b) by using the Van't Hoff equation:

$$\ln K_d = \frac{\Delta S°}{R} - \frac{\Delta H°}{RT} \tag{15}$$

$$K_d \text{ (mL/g)} = \left(\frac{C_0 - C_e}{C_e}\right) \times \frac{V}{m} \tag{16}$$

The values of $\Delta G°$ were determined using the following equation:

$$\Delta G° = -RT \ln K_d \tag{17}$$

The values of thermodynamic parameters for Cr(VI) adsorption onto PGP-1N H$_2$SO$_4$ are given in Table 6. The value of $\Delta H°$ was found to be positive (31.08 kJ/mol), which designated the endothermic nature of the process [5,17,96]. The positive value of $\Delta S°$ (161.29 J/mol K) indicated an increase in the randomness at the solid/solution interface during the adsorption of Cr(VI) onto PGP-1N H$_2$SO$_4$ [2,5,17,96]. The negative values of $\Delta G°$ proved that the adsorption process is spontaneous and does not need any external power source. Decreasing the values of $\Delta G°$ with increasing temperature indicates the better feasibility of the adsorption at a lower temperatures [2,5,96].

3.7. Application

3.7.1. Removal of Cr(VI) from different environmental water samples

The retention of Cr(VI) from different environmental water samples was investigated using the batch technique. This work was achieved using DDW, tab water, synthetic seawater, natural seawater, and real wastewater obtained from Teraat Al Esmaieliah and Bahr El-Baqar drain and the results are given in Table 7. The percentage of Cr(VI) removal from aqueous solutions prepared by dissolving of the Cr(VI) into DDW, tab water, synthetic seawater, natural seawater, and real wastewater obtained from Teraat Al

Esmaieliah and Bahr El-Baqar drain were 96.0%, 95.55%, 94.70%, 93.65%, 91.05%, and 89.95% for PGP-1N H$_2$SO$_4$, respectively, which indicates that the% removal of Cr(VI) adsorption was a slightly affecting by the changing of the type of chromium ion solution. The slight decrease in the removal percentages and maximum capacities may be due to the competition which occurred between Na$^+$ (Which is abundant in saltwater), some of the heavy metals (which are abundant in Teraat Al Esmaieliah and Bahr El-Baqar drain), and Cr(VI) for occupying the available active sites.

3.8. Desorption and regeneration studies

Desorption is a very important process in terms of assessing the economic value of the PGP-1N H$_2$SO$_4$ sorbent material. Moreover, it also will help to regenerate the spent adsorbent so that it can be used again to adsorb metal ions, and to develop the successful sorption process [38,68]. Desorption studies were done at 25°C ± 1°C by shaking 25 mL 0.5 N different eluting agents (HCl, HNO$_3$, H$_2$SO$_4$, and NaOH) with 0.1 g PGP-1N H$_2$SO$_4$ sample loaded with Cr(VI). The order of desorption for Cr(VI) metal ions was NaOH (99.00%) > HNO$_3$ (46.87%) > HCl (23.40%) > H$_2$SO4 (9.87%). The better recovery of Cr(VI) metal ions was achieved using 0.5 N NaOH giving 99.00% desorption after 180 min contact time. Activation of the washed PGP-1N H$_2$SO$_4$ after the desorption process was achieved by agitation with 1N HNO$_3$ for 180 min followed by washing with DDW.

4. Conclusion

- The present study shows that the chemically treated pomegranate peel (PGP-1N H$_2$SO$_4$) is an efficient adsorbent for the retention of Cr(VI) ions from polluted solutions.
- Characterization of the prepared adsorbent was achieved via FT-IR, SEM, TGA, and XRD analyses.
- The optimized conditions for Cr(VI) removal was attained at pH 3.0, adsorbent dose 4 g/L, concentration 400 mg/L, and contact time of 180 min.
- The pseudo-second-order equation represented the better adsorption kinetics for the adsorption of Cr(VI) onto PGP-1N H$_2$SO$_4$.
- The isotherm equilibrium studies confirmed that the Langmuir model is the best suitable model for representing the adsorption of Cr(VI) by PGP-1N H$_2$SO$_4$ with

Table 7
Removal efficiency and maximum capacity of Cr(VI) ions from different water samples using PGP-1N H$_2$SO$_4$ (4.0 g/L)

Sample			Removal (%)	Maximum capacity (mg/g)
No.	Type	pH		
1	Double-distilled water (DDW)	3.00	96.00	18.00
2	Tap water	3.00	95.55	17,91
3	Synthetic sea water	3.00	94.70	17.76
4	Natural sea water	3.00	93.65	17.56
5	Wastewater (Teraat Al Esmaieliah)	3.00	91.05	17.07
6	Wastewater (Bahr El-Baqar drain)	3.00	89.95	16.87

maximum monolayer adsorption capacity (q_e) equal to 28.28 mg/g at 25°C ± 1°C.

- The adsorption capacity of PGP-1N H_2SO_4 is much better than other adsorbents.
- The negative values of $\Delta G°$ suggested the spontaneous nature of Cr(VI) adsorption onto PGP-1N H_2SO_4, while the positive value of $\Delta H°$ and $\Delta S°$ indicated the endothermic adsorption process and Cr(VI) adsorption caused the randomness in the system.
- The desorption results showed that the best recovery for Cr(VI) metal ions was achieved using 0.5 N NaOH.

References

[1] V.K. Gupta, M. Gupta, S. Sharma, Process development for the removal of lead and chromium from aqueous solutions using red mud–an aluminium industry waste, Water Res., 35 (2001) 1125–1134.

[2] A. Ali, K. Saeed, F. Mabood, Removal of chromium(VI) from aqueous medium using chemically modified banana peels as efficient low-cost adsorbent, Alex. Eng. J., 66 (2016) 2933–2942.

[3] A. Alemu, B. Lemma, N. Gabbiye, M. Tadele, M. Teferi, Removal of chromium(VI) from aqueous solution using vesicular basalt: a potential low cost wastewater treatment system, Heliyon, 4 (2018) e00712, doi: 10.1016/j.heliyon.2018.e00682.

[4] F.C. Richard, A.C. Bourg, Aqueous geochemistry of chromium: a review, Water Res., 25 (1991) 807–816.

[5] G. Sharma, M. Naushad, A.H. Al-Muhtaseb, A. Kumar, M.R. Khan, S. Kalia, Shweta, M. Bala, A. Sharma, Fabrication and characterization of chitosan-crosslinked-poly(alginic acid) nanohydrogel for adsorptive removal of Cr(VI) metal ion from aqueous medium, Int. J. Biol. Macromol., 95 (2017) 484–493.

[6] C.E. Barrera-Diaz, V. Lugo-Lugo, B. Bilyeu, A review of chemical, electrochemical and biological methods for aqueous Cr(VI) reduction, J. Hazard. Mater., 223 (2012) 1–12.

[7] P.M. Jardine, S.E. Fendorf, M.A. Mayes, I.L. Larsen, S.C. Brooks, W.B. Bailey, Fate and transport of hexavalent chromium in undisturbed heterogeneous soil, Environ. Sci. Technol., 33 (1999) 2939–2944.

[8] S.S. Poguberović, D.M. Krčmar, S.P. Maletić, Z. Kónya, D.D.T. Pilipović, D.V. Kerkez, S.D. Rončević, Removal of As(III) and Cr(VI) from aqueous solutions using "green" zero-valent iron nanoparticles produced by oak, mulberry and cherry leaf extracts, Ecol. Eng., 90 (2016) 42–49.

[9] M. Pepi, F. Baldi, Modulation of chromium(VI) toxicity by organic and inorganic sulfur species in yeasts from industrial wastes, Biometals, 5 (1992) 179–185.

[10] M. Gheju, Hexavalent chromium reduction with zero-valent iron (ZVI) in aquatic systems, Water Air Soil Pollut., 222 (2011) 103–148.

[11] J. Němeček, P. Pokorný, O. Lhotský, V. Knytl, P. Najmanová, J. Steinová, M. Černík, A. Filipová, J. Filip, T. Cajthaml, Combined nano-biotechnology for in-situ remediation of mixed contamination of groundwater by hexavalent chromium and chlorinated solvents, Sci. Total Environ., 563–564 (2016) 822–834.

[12] A. Kumar, G. Sharma, G. Chengsheng, M. Naushad, D. Pathania, P. Dhiman, S. Kalia, Magnetically recoverable ZrO_2/Fe_3O_4/chitosan nanomaterials for enhanced sunlight driven photoreduction of carcinogenic Cr(VI) and dechlorination & mineralization of 4-chlorophenol from simulated waste water, RSC Adv., 6 (2016) 13251–13263.

[13] A.G. Williams, M.M. Scherer, Kinetics of Cr(VI) reduction by carbonate green rust, Environ. Sci. Technol., 35 (2001) 3488–3494.

[14] A.K. Shanker, C. Cervantes, H. Loza-Tavera, S. Avudainayagam, Chromium toxicity in plants, Environ. Int., 31 (2005) 739–753.

[15] Y. Hojo, Y. Satomi, In vivo nephrotoxicity induced in mice by chromium(VI), Biol. Trace Elem. Res., 31 (1991) 21–31.

[16] K.H. Cheung, J.D. Gu, Mechanism of hexavalent chromium detoxification by microorganisms and bioremediation

[17] Z.A. Al-Othman, R. Ali, M. Naushad, Hexavalent chromium removal from aqueous medium by activated carbon prepared from peanut shell: adsorption kinetics, equilibrium and thermodynamic studies, Chem. Eng. J., 184 (2012) 238–247.

[18] O.N. Kononova, G.L. Bryuzgina, O.V. Apchitaeva, Y.S. Kononov, Ion exchange recovery of chromium(VI) and manganese(II) from aqueous solutions, Arabian J. Chem., 12 (2019) 2713–2720.

[19] G.S. Fomin, Water: A Control of Chemical, Bacterial and Radiation Safety according to International Standards, Protector, Moscow, 2010.

[20] C.F. Carolin, P.S. Kumar, A. Saravanan, G.J. Joshiba, M. Naushad, Efficient techniques for the removal of toxic heavy metals from aquatic environment: a review, J. Environ. Chem. Eng., 5 (2017) 2782–2799.

[21] D. Park, Y.S. Yum, J.Y. Kim, J.M. Park, How to study Cr(VI) biosorption: use of fermentation waste for detoxifying Cr(VI) in aqueous solution, Chem. Eng. J., 136 (2008) 173–179.

[22] D. Petruzzelli, R. Passino, G. Tiravanti, Ion exchange process for chromium removal and recovery from tannery wastes, Ind. Eng. Chem. Res., 34 (1995) 2612–2617.

[23] S. Rengaraj, K.H. Yeon, S.H. Moon, Removal of chromium from water and wastewater by ion exchange resins, J. Hazard. Mater., 87 (2001) 273–287.

[24] P. Gao, P. Chen, F. Shen, G. Chen, Removal of chromium(VI) from wastewater by combined electrocoagulation-electrofloatation without a filter, Sep. Purif. Technol., 43 (2005) 117–123.

[25] C.A. Kozlowski, W. Walkowiak, Removal of chromium(VI) from aqueous solutions by polymer inclusion membranes, Water Res., 36 (2002) 4870–4876.

[26] L. Ge, B. Wu, Q. Li, Y. Wang, D. Yu, L. Wu, J. Pan, J. Miao, T. Xu, Electrodialysis with nanofiltration membrane (EDNF) for high-efficiency cations fractionation, J. Membr. Sci., 498 (2016) 192–200.

[27] H. Moloukhia, W.S. Hegazy, E.A. Abdel-Galil, S.S. Mahrous, Removal of Eu^{3+}, Ce^{3+}, Sr^{2+}, and Cs^+ ions from radioactive waste solutions by modified activated carbon prepared from coconut shells, Chem. Ecol., 32 (2016) 324–345.

[28] E.A. Abdel-Galil, H.E. Rizk, W.M. El-kenany, Low cost natural adsorbent for removal of Pb(II) ions from waste solutions, Arabian J. Nucl. Sci. Appl., 51 (2018) 19–30.

[29] M. Naushad, T. Ahamad, B.M. Al-Maswari, A.A. Alqadami, S.M. Alshehri, Nickel ferrite bearing nitrogen-doped mesoporous carbon as efficient adsorbent for the removal of highly toxic metal ion from aqueous medium, Chem. Eng. J., 330 (2017) 1351–1360.

[30] J. Kyziol-Komosinska, C. Rosik-Dulewska, A. Dzieniszewska, M. Pajâk, I. Krzyzewska, Removal of Cr(III) ions from water and wastewater by sorption onto peats and clays occurring in an overburden of lignite beds in Central Poland, Environ. Prot. Eng., 40 (2014) 5–22.

[31] A. Sdiri, T. Higashi, T. Hatta, F. Jamoussi, N. Tase, Evaluating the adsorptive capacity of montmorillonitic and calcareous clays on the removal of several heavy metals in aqueous systems, Chem. Eng. J., 172 (2011) 37–46.

[32] M. Kobya, Adsorption kinetic and equilibrium studies of Cr(VI) by hazelnut shell activated carbon, Adsorpt. Sci. Technol., 22 (2004) 51–64.

[33] K. Kadirvelu, M. Kavipriya, C. Karthika, M. Radhika, N. Vennilamani, S. Pattabhi, Utilization of various agricultural wastes for activated carbon preparation and application for the removal of dyes and metal ions from aqueous solution, Bioresour. Technol., 87 (2003) 129–132.

[34] G. Moussavi, B. Barikbin, Biosorption of chromium(VI) from industrial wastewater onto pistachio hull waste biomass, Chem. Eng. J., 162 (2010) 893–900.

[35] K. Wang, G. Qiu, H. Cao, R. Jin, Removal of chromium(VI) from aqueous solutions using Fe_3O_4 magnetic polymer microspheres functionalized with amino groups, Materials, 8 (2015) 8378–8391.

[36] E. Alemayehu, S.T. Bruhnb, B. Lennartza, Adsorption behaviour of Cr(VI) onto macro and micro-vesicular volcanic rocks from water, Sep. Purif. Technol., 78 (2011) 55–61.

application potential: a review, Int. Biodeterior. Biodegrad., 59 (2007) 8–15.

[37] M.R. Moghadam, N. Nasirizadeh, Z. Dashti, E. Babanezhad, Removal of Fe(II) from aqueous solution using pomegranate peel carbon: equilibrium and kinetic studies, Int. J. Ind. Chem., 4 (2013) 4–19.

[38] A.E. Nemr, Potential of pomegranate husk carbon for Cr(VI) removal from wastewater: kinetic and isotherm studies, J. Hazard. Mater., 161 (2009) 132–141.

[39] M. Alam, R. Nadeem, M.I. Jilani, Pb(II) removal from wastewater using pomegranate waste biomass, Int. J. Chem. Biochem. Sci., 1 (2012) 24–29.

[40] M. Ghaedi, H. Tavallali, M. Sharifi, S.N. Kokhdan, A. Asghari, Preparation of low cost activated carbon from *Myrtus communis* and pomegranate and their efficient application for removal of congo red from aqueous solution, Spectrochim. Acta, Part A, 86 (2012) 107–114.

[41] S. Kamel, H. Abou-Yousef, M. Yousef, M. El-Sakhawy, Potential use of bagasse and modified bagasse for removing of iron and phenol from water, Carbohydr. Polym., 88 (2012) 250–256.

[42] W.S. Nagh, M.A.K.M. Hanafiah, Removal of heavy metal ions from wastewater by chemically modified plant wastes as adsorbents: a review, Bioresour. Technol., 99 (2008) 3935–3948.

[43] E.S. Abdel-Halim, S.S. Al-Deyab, Chemically modified cellulosic adsorbent for divalent cations removal from aqueous solutions, Carbohydr. Polym., 87 (2012) 1863–1868.

[44] H. Kamandari, H. Hashemipour, L. Saeednia, H. Najjarzadeh, Experimental and modeling study on the production of activated carbon from pistachio shells in rotary reactor, Res. Chem. Intermed., 40 (2014) 509–521.

[45] H. Deng, G. Zhang, X. Xu, G. Tao, J. Dai, Optimization of preparation of activated carbon from cotton stalk by microwave assisted phosphoric acid-chemical activation, J. Hazard. Mater., 182 (2010) 217–224.

[46] S. Chowdhury, S. Chakraborty, P. Saha, Biosorption of basic green 4 from aqueous solution by *Ananas comosus* (pineapple) leaf powder, Colloids Surf., B, 84 (2011) 520–527.

[47] N. Kannan, M.M. Sundaram, Kinetics and mechanism of removal of methylene blue by adsorption on various carbons–a comparative study, Dyes Pigm., 51 (2001) 25–40.

[48] T.A. Saleh, V.K. Gupta, Functionalization of tungsten oxide into MWCNT and its application for sunlight induced degradation of rhodamine B, J. Colloid Interface Sci., 362 (2011) 337–344.

[49] N.H.M. Nayan, S.I.A. Razak, W.A.W.A. Rahman, R.A. Majid, Effects of mercerization on the properties of paper produced from Malaysian pineapple leaf fiber, Int. J. Eng. Technol., 13 (2013) 1–6.

[50] M. Maniruzzaman, M.A. Rahman, M.A. Gafur, H. Fabritius, D. Raabe, Modification of pineapple leaf fibers and graft copolymerization of acrylonitrile onto modified fibers, J. Compos. Mater., 46 (2012) 79–90.

[51] E.A. Abdel-Galil, H.E. Rizk, A.Z. Mostafa, Production and characterization of activated carbon from Leucaena plant wastes for removal of some toxic metal ions from waste solutions, Desal. Water Treat., 57 (2016) 17880–17891.

[52] T.A. Saleh, M.N. Siddiqui, A.A. Al-Arfaj, Synthesis of multiwalled carbon nanotubes-titania nanomaterial for desulfurization of model fuel, J. Nanomater., 2014 (2014) 1–6.

[53] A. Sallam, M.S. Al-Zahrani, M.I. Al-Wabel, A.S. Al-Farraj, A.R.A. Usman, Removal of Cr(VI) and toxic ions from aqueous solutions and tannery wastewater using polymer-clay composites, Sustainability, 9 (2017) 1–14.

[54] E.A. Abdel-Galil, H. Moloukhia, M. Abdel-Khalik, S.S. Mahrous, Synthesis and physico-chemical characterization of cellulose/HO$_7$Sb$_3$ nanocomposite as adsorbent for the removal of some radionuclides from aqueous solutions, Appl. Radiat. Isotopes, 140 (2018) 363–373.

[55] M.R. Gandhi, S. Meenakshi, Preparation and characterization of La(III) encapsulated silica gel/chitosan composite and its metal uptake studies, J. Hazard. Mater., 203 (2012) 29–37.

[56] R. Karthik, S. Meenakshi, Removal of hexavalent chromium ions using polyaniline/silica gel composite, J. Water Process Eng., 1 (2014) 37–45.

[57] S. Vivekanandhan, L. Christensen, M. Misra, A.K. Mohanty, Green process for impregnation of silver nanoparticles into microcrystalline cellulose and their antimicrobial bio-nanocomposite films, J. Biomater. Nanobiotechnol., 3 (2012) 371–376.

[58] A.P. Mathew, K. Oksman, M. Sain, Mechanical properties of biodegradable composites from poly lactic acid (PLA) and microcrystalline cellulose (MCC), J. Appl. Polym. Sci., 97 (2005) 2014–2025.

[59] U. Guyo, J. Mhonyera, M. Moyo, Pb(II) adsorption from aqueous solutions by raw and treated biomass of maize stover—a comparative study, Process Saf. Environ. Prot., 93 (2015) 192–200.

[60] M. Naushad, Surfactant assisted nano-composite cation exchanger: development, characterization and applications for the removal of toxic Pb^{2+} from aqueous medium, Chem. Eng. J., 235 (2014) 100–108.

[61] M.M. Hamed, A.M. Shahr El-Din, E.A. Abdel-Galil, Nanocomposite of polyaniline functionalized tafla: synthesis, characterization, and application as a novel sorbent for selective removal of Fe(III), J. Radioanal. Nucl. Chem., 322 (2019) 663–676.

[62] Y. Li, Q. Du, X. Wang, P. Zhang, D. Wang, Z. Wang, Y. Xia, Removal of lead from aqueous solution by activated carbon prepared from *Enteromorpha prolifera* by zinc chloride activation, J. Hazard. Mater., 183 (2010) 583–589.

[63] V. Gupta, A. Rastogi, Biosorption of lead from aqueous solutions by green algae *Spirogyra* species: kinetics and equilibrium studies, J. Hazard. Mater., 152 (2008) 407–414.

[64] S. Lagergren, Zurtheorie der sogenannten adsorption geloster stoffe, Kungl. Svens. Vetenskapsakad. Handl., 24 (1898) 1–39.

[65] Y.S. Ho, G. McKay, The sorption of lead(II) ions on peat, Water Res., 33 (1999) 578–584.

[66] Y.S. Ho, G. Mckay, The kinetics of sorption of divalent metal ions onto sphagnum moss peat, Water Res., 34 (2000) 735–742.

[67] S.H. Chien, W.R. Clayton, Application of Elovich equation to the kinetics of phosphate release and sorption in soils, Soil Sci. Soc. Am. J., 44 (1980) 265–268.

[68] X. Huang, Y. Liu, S. Liu, X. Tan, Y. Ding, G. Zeng, Y. Zhou, M. Zhang, S. Wang, B. Zhengd, Effective removal of Cr(VI) using β-cyclodextrin–chitosan modified biochars with adsorption/reduction bifuctional roles, RSC Adv., 6 (2016) 94–104.

[69] S. Goswami, U.C. Ghosh, Studies on adsorption behavior of Cr(VI) onto synthetic hydrous stannic oxide, Water SA, 31 (2005) 597–602.

[70] W.J. Weber, J.C. Morris, Kinetics of adsorption on carbon from solution, J. Sanit. Eng. Div., 89 (1963) 31–60.

[71] D.P. Dutta, S. Nath, Low cost synthesis of SiO$_2$/C nanocomposite from corn cobs and its adsorption of uranium(VI), chromium(VI) and cationic dyes from wastewater, J. Mol. Liq., 269 (2018) 140–151.

[72] I. Langmuir, The adsorption of gases on plane surfaces of glass, mica and platinum, J. Am. Chem. Soc., 40 (1918) 1361–1403.

[73] K.R. Hall, L.C. Eagleton, A. Acrivos, T. Vermeulen, Pore- and solid-diffusion kinetics in fixed-bed adsorption under constant-pattern conditions, Ind. Eng. Chem. Fundam., 5 (1966) 212–223.

[74] E.A. Abdel-Galil, R.S. Hassan, M.A. Eid, Assessment of nano-sized stannic silicomolybdate for the removal of ^{137}Cs, ^{90}Sr, and ^{141}Ce radionuclides from radioactive waste solutions, Appl. Radiat. Isotopes, 148 (2019) 91–101.

[75] M. Bhaumik, A. Maity, V.V. Srinivasu, M.S. Onyango, Removal of hexavalent chromium from aqueous solution using polypyrrole-polyaniline nanofibers, Chem. Eng. J., 181–182 (2012) 323–333.

[76] X. Dong, L.Q. Ma, Y. Li, Characteristics and mechanisms of hexavalent chromium removal by biochar from sugar beet tailing, J. Hazard. Mater., 190 (2011) 909–915.

[77] D. Mohan, K.P. Singh, V.K. Singh, Removal of hexavalent chromium from aqueous solution using low-cost activated carbons derived from agricultural waste materials and activated carbon fabric cloth, Ind. Eng. Chem. Res., 44 (2005) 1027–1042.

[78] N. Vennilamini, K. Kadirvelu, Y. Sameena, S. Patabhi, Utilization of activated carbon prepared from industrial solid waste for the removal of Cr(VI) ions from synthetic and industrial effluent, Adsorpt. Sci. Technol., 23 (2005) 145–160.

[79] A. Bhattacharya, T. Naiya, S. Mandal, S. Das, Adsorption, kinetics and equilibrium studies on removal of Cr(VI) from aqueous solutions using different low-cost adsorbents, Chem. Eng. J., 137 (2008) 529–554.

[80] M. Dakiky, M. Khamis, M. Manassra, M. Mer'eb, Selective adsorption of Chromium(VI) in industrial waste water using low cost abundantly available adsorbents, Adv. Environ. Res., 6 (2002) 533–540.

[81] N.K. Hamadi, X.D. Chen, M.M. Farid, M.G.Q. Lu, Adsorption kinetics for the removal of chromium(VI) from aqueous solution by adsorbents derived from used tyres and sawdust, J. Chem. Eng., 84 (2001) 95–105.

[82] A. Namasivayam, K. Ranganathan, Waste Fe(III)/Cr(III) hydroxide as adsorbent for the removal of Cr(VI) from aqueous solution and chromium plating industry wastewater, Environ. Pollut., 82 (1993) 255–261.

[83] H. Singh, V.K. Rattan, Comparison of hexavalent chromium adsorption from aqueous solutions by various biowastes and granulated activated carbon, Indian Chem. Eng., 56 (2014) 12–28.

[84] M. Nameni, M.R. Alavi Moghadam, M. Arami, Adsorption of hexavalent chromium from aqueous solutions by wheat bran, Int. J. Environ. Sci. Technol., 5 (2008) 161–168.

[85] G. Cimino, A. Passerini, G. Toscano, Removal of toxic cations and Cr(VI) from aqueous solution by hazelnut shell, Water Res., 34 (2000) 2955–2962.

[86] D.C. Sharma, C.F. Forster, A Preliminary examination into the adsorption of hexavalent chromium using low-cost adsorbents, Bioresour. Technol., 47 (1994) 257–264.

[87] W.T. Tan, S.T. Ooi, C.K. Lee, Removal of chromium(VI) from solution by coconut husk and palm pressed fibres, Environ. Technol., 14 (1993) 277–282.

[88] Y. Orhan, H. Buyukgungur, The removal of heavy metals by using agricultural wastes, Water Sci. Technol., 28 (1993) 247–255.

[89] M.E. Argun, S. Dursun, C. Ozdemir, M. Karatas, Heavy metal adsorption by modified oak sawdust: thermodynamics and kinetics, J. Hazard. Mater., 141 (2007) 77–85.

[90] H.M.F. Freundlich, Over the adsorption in solution, J. Phys. Chem., 57 (1906) 385–470.

[91] G.O. Wood, Affinity coefficients of the Polanyi/Dubinin adsorption isotherm equations: a review with compilations and correlations, Carbon, 39 (2001) 343–356.

[92] A. Agrawal, C. Pal, K. Sahu, Extractive removal of chromium(VI) from industrial waste solution, J. Hazard. Mater., 159 (2008) 458–464.

[93] M.M. Dubinin, The potential theory of adsorption of gases and vapors for adsorbents with energetically non-uniform surface, Chem. Rev., 60 (1960) 235–266.

[94] J.P. Hobson, Physical adsorption isotherms extending from ultra-high vacuum to vapor pressure, J. Phys. Chem., 73 (1969) 2720–2727.

[95] M. Naushad, S. Vasudevan, G. Sharma, A. Kumar, Z.A. Al-Othman, Adsorption kinetics, isotherms, and thermodynamic studies for Hg^{2+} adsorption from aqueous medium using alizarin red-S-loaded amberlite IRA-400 resin, Desal. Water Treat., 57 (2016) 18551–18559.

[96] A.A. Alqadami, M. Naushad, Z.A. Al-othman, A.A. Ghfar, Novel metal−organic framework (MOF) based composite material for the sequestration of U(VI) and Th(IV) metal ions from aqueous environment, ACS Appl. Mater. Interface, 9 (2017) 36026–36037.